RSC Advances

PAPER

View Article Online
View Journal | View Issue

Cite this: *RSC Adv.*, 2023, **13**, 22268

Curcumin nanoparticles: physicochemical fabrication, characterization, antioxidant, enzyme inhibition, molecular docking and simulation studies

Qudsia Kanwal, †*[a] Mahmood Ahmed, †*[b] Muhammad Hamza,[ac] Muhammad Ahmad,[b] Atiq-ur-Rehman,[d] Numan Yousaf,[e] Arshad Javaid,[f] Aneela Anwar,[g] Iqra Haider Khan[f] and Muhammad Muddassar *[e]

Curcumin is an extensively studied natural compound due to its extensive biological applications. However, there are some drawbacks linked to this compound such as poor absorption, low water-solubility, quick systemic elimination, fast metabolism, poor pharmacokinetics, low bioavailability, low penetration targeting efficacy and low stability. To overcome these drawbacks, curcumin is encapsulated in nano-carriers. In the current studies, we synthesized nanoparticles of curcumin without using nanocarriers by different methods such as nano-suspension (Cur-NSM), sonication (Cur-SM) and anti-solvent precipitation (Cur-ASP) to enhance the solubility of curcumin in water. The prepared nanoparticles were characterized by FTIR, SEM and XRD analysis. These curcumin nanoparticles were screened for their solubilities in water, DPPH scavenging, amylase, α-glucosidase and β-glucosidase enzymatic activities. The particle size of nano-curcumin was found to be in the 47.4–98.7 nm range. The reduction in particle size of curcumin dramatically increases its solubility in water to 79.2 μg mL^{-1}, whereas the solubility of curcumin is just 0.98 μg mL^{-1}. Cur-ASP showed the highest free radical scavenging potential (48.84 ± 0.98%) which was comparable with standard BHT (50.48 ± 1.11%) at 75.0 μg mL^{-1}. As well, Cur-ASP showed the highest inhibition of α-amylase (68.67 ± 1.02%), α-glucosidase (58.30 ± 0.52%), and β-glucosidase (64.80 ± 0.43%) at 100 μg mL^{-1} which is comparable with standard drug acarbose. The greater surface area of nanoparticles exposes the various groups of curcumin for blocking the binding sites of enzymes. This strategy may be helpful in designing curcumin as a potent therapeutic agent against diabetes mellitus. Further, the molecular interactions of curcumin with α-amylase, α-glucosidase, β-glucosidase, and polyphenol oxidase were assessed by analyzing the plausible binding modes of curcumin in the binding pocket of each receptor. The best binding mode of curcumin was used to make complexes with the target proteins and their stability was confirmed by 50 ns MD simulation.

Received 3rd March 2023
Accepted 17th July 2023

DOI: 10.1039/d3ra01432k

rsc.li/rsc-advances

1. Introduction

Curcumin (diferuloylmethane) is a naturally occurring compound present in turmeric which demonstrates some really important medicinal properties (*Curcuma longa* L.). Due to its anti-inflammatory and antioxidant behavior, it has been playing a significant role in the treatment of different pathological diseases like diabetes, cancer, Alzheimer's disease, cardiovascular disease, neurological disorders, cancer, tumors and inflammatory disorders.[1–6] In spite of its extraordinary pharmaceutical applications, the clinical application of curcumin is limited due to its low solubility, poor bioavailability, physicochemical instability, poor pharmacokinetics, and fast metabolism.[7–9] However, such issues can be addressed and overcome by using an effective target specific drug delivery system. To improve the pharmacokinetics and bioavailability of curcumin, nano-formulations have been reported which may be launched as a drug after effective accomplishment of pre-clinical and clinical trials.[10–14]

[a]*Department of Chemistry, The University of Lahore, Lahore, Pakistan. E-mail: qudsia.kanwal@chem.uol.edu.pk*

[b]*Department of Chemistry, Division of Science and Technology, University of Education, College Road, Lahore, Pakistan. E-mail: mahmoodresearchscholar@gmail.com; mahmood.ahmed@ue.edu.pk*

[c]*Additive Manufacturing Institute, Shenzhen University, China*

[d]*Department of Pharmacy, The University of Lahore, Lahore, Pakistan*

[e]*Department of Biosciences, COMSATS University Islamabad, Islamabad, Pakistan*

[f]*Institute of Agricultural Sciences, University of the Punjab, Lahore, Pakistan*

[g]*Basic Sciences and Humanity, University of Engineering and Technology, Kala Shah Kaku Campus, Lahore, Pakistan*

† These authors contributed equally to this work.

Diabetes mellitus type 2 (DM) is a complex non-communicable disease linked to the dysfunction of pancreatic cells and resistance to insulin leading to postprandial hyperglycemia.[15,16] Due to enhanced consumption of carbohydrate and modern lifestyle with less physical effort, this disease has become a global health challenge as well as economic burden. Due to cost effective management of DM in developing countries, the frequency may worsen, with a substantial effect on the population of developing countries. The diabetic condition, when not properly treated, develops to chronic hyperglycemia. It would increase the rate of production of non-mitochondrial and mitochondrial reactive oxygen species (ROS). This phenomenon helps to accelerate the activation of protein kinase C (PKC) isoforms, polyol pathway flux, hexosamine pathway flux and advanced glycation end products involved in the hyper glycaemia-induced oxidative damage followed by, enhanced ROS production. This enhanced ROS has negative impact on insulin regulation signaling resulting in insulin resistance, impaired glucose tolerance, mitochondrial dysfunction and cell dysfunction.[17–19] Reduction of insulin gene expression takes place due to the interaction of ROS with pancreatic cells and due to low level of antioxidant enzymes, hence results in reduction in insulin secretion.[20] One of the major therapeutic targets recently reported for type 2 DM management is to control the glucose reabsorption in intestine. For this purpose, inhibition of glucose hydrolyzing enzymes like amylase and glucosidase is necessary.[21–23] The alpha-amylase (-1,4-glucan-4-glucanohydrolases) is the most prominent enzyme as secretory product of salivary gland and that of pancreas. It is responsible for the conversion of mixture of complex carbohydrates to oligosaccharides and disaccharides by hydrolysis. The oligosaccharides produced were further hydrolyzed by glucosidase to terminal glucose monosaccharide units. The existing inhibitors of alpha-amylase and glucosidase enzymes used for the clinical treatment of DM have wide range of side effects such as diarrhea hypoglycemia, bowel bloating and flatulence which limits their use.[24] There is, therefore, an urgent need to look for less toxic alternatives for the management of DM. Dietary intake from herbal source with high antioxidants potentials has exhibited a wonderful beneficial impact on pancreatic cells in diabetic condition by deferring or stopping beta cells dysfunction against glucose toxicity.[25,26]

Within the context of above study, a comparative mechanistic approach should be applied to know that how the curcumin nano-formulations enhance the therapeutic activity as compared to native curcumin. How the nano-curcumin may control the progression, recurrence, metastases, and disorder of diseases. The nano-curcumin may provide greater surface area to expose its OH groups on the surface of molecule. Thus, individual molecule becomes significantly solubilized by solvation after developing hydrogen bonding with water molecules to enhance the solubility and hence bioavailability of these compounds. Hence, a lower amount of dose will be required for target specific curcumin nanoparticles delivery to reduce the side effects of a specific dose and thus to restrict the binding sides of enzymes to reduce the glucose toxicity. Additionally, current developments have shown that a nano-formulation of drug controls the microenvironment and provides a better therapeutic index. Hence, by developing nano-curcumin would solve many diseases related problems and being the part of our diet may help to facilitate patient by reducing cost, and side effects, and by increasing potential benefits. The overall aim of this study is the fabrication of curcumin nanoparticles by different methods to enhance the solubility of curcumin in water and to make it bioavailable for human body. Furthermore, the present study investigates the antioxidant and antidiabetic activities, and *in silico* studies were performed to check the role of curcumin as ligands against the α-amylase, α-glucosidase, β-glucosidase, and polyphenol oxidase enzymes by molecular docking studies. The stability of curcumin with the said enzymes was also confirmed by analyzing the MD trajectories generated by 50 ns simulation.

2. Experimental

2.1. Chemicals

HPLC grade ethanol and *n*-hexane (Panreac, Barcelona, Spain) were acquired from Hajvery Scientific Store, Lahore-Pakistan. The GenPure (Thermo Scientific, USA) water system was used to prepare ultrapure water (18 MΩ cm resistivity).

2.2. Fabrication of curcumin nanoparticles

Curcumin nanoparticles were prepared using three methods for its enhanced solubility such as evaporation through nano-suspension method (NSM), sonication method (SM) and anti-solvent precipitation method (ASP). The particles obtained from these methods were named as Cur-NSM, Cur-SM and Cur-ASP respectively.

2.2.1. Nano-suspension method. This method was adopted with slight modification in reported method.[27] Briefly, the ethanoic solution of curcumin (5 mg mL^{-1}) was added rapidly to *n*-hexane under constant stirring. A nano-suspension was formed rapidly by adding antisolvent to this ethanolic solution. For 20 mL of ethanoic solution of curcumin, 300 mL of *n*-hexane (1 : 15) was used. This suspension mixture was subjected to a rapid evaporation under vacuum using rotary evaporator. The obtained suspension was freeze-dried under vacuum.

2.2.2. Sonication method. A partially modified method[28] was used for the synthesis of nanoparticles of curcumin. For this purpose, the stock solution of curcumin was prepared in ethanol (15 mg mL^{-1}) then dropwise addition of this stock solution (1 mL) was carried out to boiling water (50.0 mL) at flow rate of 0.1 mL min^{-1} in a sonicator under ultra-sonication conditions (Velp Scientifica Srl, Italy). After 30 min of sonication, the mixture was stirred for 30 min at 800 rpm. Bright orange-colored precipitates were obtained in a suspension. After formation of suspension, the mixture was kept in freeze-dryer for 24 h at −18 °C and the solvent was removed by freeze dryer.

2.2.3. Anti-solvent precipitation method. This method was adopted with slight modification in reported method.[27] Briefly, the ethanoic solution of curcumin (5 mg mL^{-1}) was prepared. The solution was added to the deionized water at fixed flow rate (1 mL min^{-1}), under constant magnetic stirring using dropping funnel. For 200 mL deionized water, curcumin solution (20 mL) in ethanol was used at 1 : 10 v/v ratio of ethanol : water. Nano suspension of curcumin was obtained, which was subjected to centrifugation at the rate of 20 000 rpm for 15 min. The curcumin nanoparticles were vacuum dried after filtration.

2.3. Characterization of nano-curcumin

Nano-curcumin were characterized for their particles size and surface morphology using SEM, XRD, FTIR and UV/Visible spectrophotometry. The absorbance spectra were recorded using UV-visible spectrophotometry (U-2910, Hitachi, Japan) ranging from of 200 to 800 nm wavelengths. X-ray powder diffractometer (Bruker D8 ADVANCE Eco) was used to record diffraction pattern with Kα (Cu) radiation (λ = 0.154 nm). These radiations were incident at 1° angle with interval of 2θ, FTIR (Bruker alpha-II) spectrophotometer with smart diamond crystal ATR was used to scan samples of nano-curcumin at wavenumber ranging from 4000 to 500 cm^{-1} to identify the chemical composition and bonding present. SEM machine (HITACHI S-3400N) was employed for surface morphological investigation of newly synthesized nanoparticles. The SEM instrument was operated at emission current of 60 μA and acceleration voltage was kept as 10 kV.

2.4. Solubility studies of nano-curcumin in water

Saturated solution of each nano-curcumin (Cur-NSM, Cur-SM and Cur-ASP) as well of pure curcumin (Cur) was prepared separately in deionized water (30 mL) under constant stirring at room temperature for 24 h. After 24 h, the mixture was centrifuged for the removal of undissolved particles followed by filtration using PTFE membrane (Merck, Germany). Each filtrate was diluted with equal amount of deionized water. The amount of dissolved curcumin was determined using UV/Visible spectrophotometer (U-2910, Hitachi, Japan) at 422 nm.

2.5. 1,1-Diphenyl-2-picrylhydrazyl (DPPH)-2,2-diphenyl-1-picrylhydrazyl free radical scavenging assay

Free radical scavenging activity (FRSA) was calculated using methanol solution of DPPH.[29–31] 15–75 μm mL^{-1} of each nano-curcumin sample was mixed with 3.0 mL of methanolic solution of DPPH (0.1 mM). After a vigorous shaking, the solution was allowed to stand for 30 min at room temperature in the dark. The absorbance was measured at 515 nm and scavenging activity was calculated using the following equation.

$$\%\ \text{FRSA} = \left[\frac{\text{Absorbance}_{\text{control}} - \text{Absorbance}_{\text{sample}}}{\text{Absorbance}_{\text{control}}}\right] \times 100$$

Butylated hydroxytoluene (BHT) was used as positive control, whereas methanol was used as negative control. BHT as well as nano-curcumin having FRSA ≥50% were examined in concentration range of 15.0, 30.0, 45.0, 60.0, and 75.0 μg mL^{-1} in DMSO to evaluate their 50% inhibitory concentration (IC_{50}) in μg mL^{-1}. The assay was performed in triplicate and IC_{50} was calculated by using GraphPad Prism 7.0 Software (Graph Pad Software Inc.).

2.6. α-Amylase inhibitory assay

Each nano-curcumin sample in a concentration ranged 20–100 μg mL^{-1} was prepared in DMSO and phosphate buffer (0.02 M, pH 6.9, 500 μL) containing of α-amylase (0.5 mg mL^{-1}) were incubated for 10 min at 25 °C whereas acarbose was used as standard drug in same manner. The blank has same volume of phosphate buffer (0.02 M) instead of nano-curcumin. After incubation substrate solution (starch 1%, 500 μL) in phosphate buffer (0.02 M) was added to reaction mixture and incubated again for 10 min at 25 °C and the reaction was stopped by addition of reagent 3,5-dinitrosalicylic acid (1 mL). Afterwards the reaction mixture was placed in water bath for 5 min in water bath at 100 °C and after cooling to room temperature the mixture was diluted with 10 mL of water. Absorbance was measured at λ_{max} 540 nm using UV/Vis spectrophotometer. Alpha-amylase inhibitory activity of different samples and the standard α-amylase inhibitor (acarbose) were calculated as follows

$$\%\ \alpha\text{-amylase inhibition} = \left[\frac{\text{Absorbance}_{\text{control}} - \text{Absorbance}_{\text{sample}}}{\text{Absorbance}_{\text{control}}}\right] \times 100$$

The assay was performed in triplicate and IC_{50} was calculated by using GraphPad Prism 7.0 Software (Graph Pad Software Inc.).

2.7. α-Glucosidase inhibition assay

This method was adopted with slight modification in reported method.[32] Rat intestinal acetone powder (1 g) was added to phosphate buffer (100 mL, pH 7.0, 0.1 M). The sonication of reaction mixture was carried out for 30 min, which was followed by centrifugation (10 000 rpm, 4 °C for 10 min.). The obtained supernatant was named as maltase enzyme/rat intestinal α-glucosidase. Each nano-curcumin sample in a concentration ranged from 20 to 100 μg mL^{-1} and solutions were made in DMSO. The phosphate buffers (0.1 M, pH 7.0, 100 μL) containing α-glucosidase (20 μL) and maltase solution (100 μL, 37 mM) were incubated for 30 min

at 37 °C, whereas acarbose was used as standard drug in same manner. The blank has same volume of phosphate buffer (0.1 M) instead of nano-curcumin. After incubation, substrate solution (*p*-nitrophenyl glucopyranoside, 25 μL) was added to reaction mixture and incubated again for 5 min at 37 °C. Absorbance was measured at λ_{max} of 400 nm using UV/Vis spectrophotometer. α-Glucosidase inhibitory activity of different samples and the standard α-glucosidase inhibitor (acarbose) were calculated as follows

$$\%\ \alpha\text{-glucosidase inhibition} = \left[\frac{\text{Absorbance}_{control} - \text{Absorbance}_{sample}}{\text{Absorbance}_{control}}\right] \times 100$$

The assay was performed in triplicate and IC_{50} was calculated by using GraphPad Prism 7.0 Software (Graph Pad Software Inc.).

2.8. β-Glucosidase inhibition assay

Each nano-curcumin sample in a concentration range of 20–100 μg mL^{-1} was prepared in DMSO and phosphate buffer (pH 5, 400 μL) containing β-glucosidase (200 μL, 20 mg mL^{-1}) were incubated for 10 min at 37 °C, whereas acarbose was used as standard drug in the same manner. The blank has same volume of phosphate buffer (0.02 M) instead of nano-curcumin. After incubation, substrate solution (*p*-nitrophenyl-β-D-glucopyranoside 200 μL, 0.2 mg mL^{-1}) in phosphate buffer was added to reaction mixture and incubated again for 30 min at 37 °C. Absorbance was measured at λ_{max} of 410 nm using UV/Vis spectrophotometer. β-Glucosidase inhibitory activity of different samples and the standard β-glucosidase inhibitor (acarbose) were calculated as follows

$$\%\ \beta\text{-glucosidase inhibition} = \left[\frac{\text{Absorbance}_{control} - \text{Absorbance}_{sample}}{\text{Absorbance}_{control}}\right] \times 100$$

The assay was performed in triplicate and IC_{50} was calculated by using GraphPad Prism 7.0 Software (Graph Pad Software Inc.).

2.9. Molecular docking and simulation studies

The molecular interactions of curcumin with α-amylase (PDB ID: 7TAA), α-glucosidase (PDB ID: 2QMJ), β-glucosidase (PDB ID: 2XWE), and polyphenol oxidase (PDB ID: 2Y9X) were analyzed by molecular docking studies. The co-crystal structures of target proteins were preprocessed in Schrodinger Maestro[33] using Protein Preparation Wizard. The structures were refined by adding hydrogens, creating disulfide, assigning bond orders, and by removing water molecules. Then PROPKA[34] was used to optimize hydrogen bonds at pH 7.0. The structures were then minimized by applying OPLS_2005 forcefield. To conduct site specific docking, a 3D grid at specific coordinates *i.e.*, (7TAA: $X = 38.85$, $Y = 39.69$, $Z = 30.46$), (2QMJ: $X = -20.82$, $Y = -6.64$, $Z = -5.24$), (2XWE: $X = -33.21$, $Y = -13.53$, $Z = 19.53$), and (2Y9X: $X = -10.02$, $Y = -28.02$, $Z = -43.6$) was generated. The curcumin was prepared by using LigPrep tool by applying OPLS_2005 forcefield. Finally, the standard precision mode of glid was used to dock the ligand with target proteins.

The binding poses of curcumin with each target were analyzed and best mode was selected for protein–ligand stability analysis at 50 ns MD simulation using VMD[35] and NAMD[36] tools. The input topology and parameter files were prepared by Ambertools 21,[37] while the ligand topology files were generated by Antechamber. The missing hydrogens in protein structures were added by using the LeaP program of ambertools. Each solvation of each complex was done in a box of 10 Å containing TIP3P water model.[38] The systems were further neutralized by adding counter Na^+ and Cl^- ions. The energy clashes of the complexes were removed by minimizing them using ff14SB and GAFF force fields for protein and ligand, respectively.[39] Finally, the solvation systems were subjected to three additional equilibrations at 200, 250, and 300 K. The equilibrated systems were then subjected to production run for 50 ns simulation and the MD trajectories were saved at every 2 ps interval. The trajectories were analyzed by BIO3D package[40] of R.

3. Results and discussion

3.1. Characterization of nano-curcumin

3.1.1. Fourier-transform infrared analysis. The FTIR spectra of curcumin and nano curcumin were recorded at IR region ranging from (4000 to 400 cm^{-1}). The spectra exhibited the IR vibrational bands (Fig. 1) corresponding to respective positions of curcumin functional groups found in curcumin and prominent in nano curcumin. An intense and strong broad band at wavenumber 3234–3361 cm^{-1} related to the vibrational frequency (stretching) of O–H bond with hydrogen bonding present in nano curcumin, but it appears as a very weak shoulder like peak in case of original pure curcumin. In case of

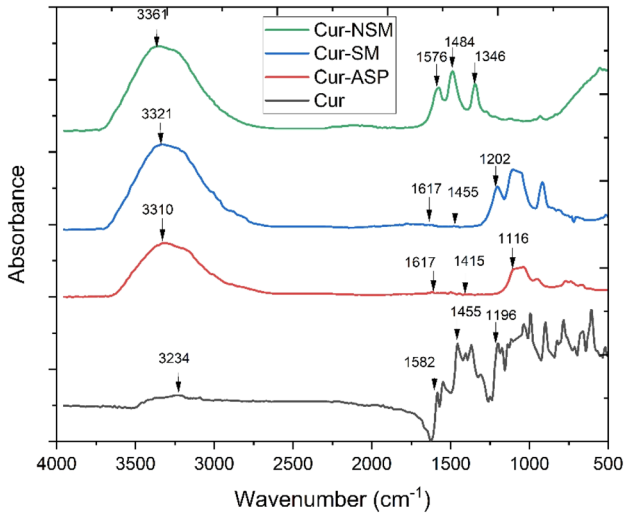

Fig. 1 Fourier-transform infrared spectrum of nano-curcumin and curcumin.

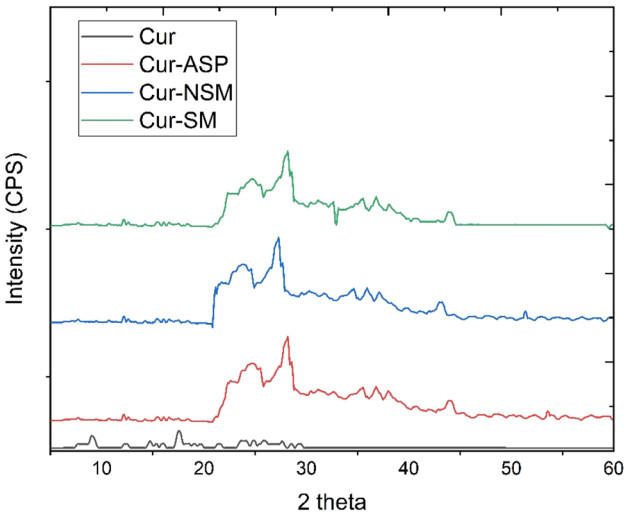

Fig. 3 X-ray diffraction pattern of nano-curcumin Cur-NSM, Cur-SM, Cur-ASP, and curcumin.

Cur-NSM and Cur-ASP, this OH stretching vibrational frequency becomes so broad and intense that Cur-SM confirms the presence of maximum hydrogen bonding. This indicates that with the reduction of the size of curcumin particles, the individual OH groups in curcumin become prominent and significant to develop hydrogen bonding. Thus, water molecules cause more solvation to yield more solubility of the curcumin molecules. As shown in Fig. 1, a weak band in the case of pure curcumin suggests almost an absence of the hydrogen bonding. A comparison of the FTIR spectra of pure and nano-curcumin indicates that a broader and intense OH band appears in the nano-curcumin spectrum, which confirms the formation of nano-curcumin. The C–H vibrational frequency appeared at 1617–1582 cm^{-1} corresponding to aromatic overtone and the peaks at 1415–1484 cm^{-1} confirm the presence of aromatic stretching frequency of the benzene ring. An intense characteristic peak was observed near 1600 cm^{-1} that is related to the C=O group conjugated with double bonded ethylene carbon vibrations. The peaks appeared at 1346 cm^{-1} and at 1116 cm^{-1} originate from the vibrational frequencies (stretching) of $C_{sp}{}^{2}$–O and $C_{sp}{}^{3}$–O bonds, respectively.

3.1.2. Scanning electron microscopic analysis. The surface morphology and nano particle size of nano-curcumin was determined using SEM analysis. The SEM spectrographs were recorded at 20k× magnification. According to SEM analysis Cur-NSM, Cur-SM and Cur-ASP exhibited cylindrical, rod like and semispherical shape (Fig. 2). The measured particle sizes of Cur-NSM, Cur-SM and Cur-ASP were 65.3 nm, 98.7 nm and 47.4 nm respectively.

3.1.3. X-ray diffraction analysis. XRD is a very strong and smart analytical technique used to evaluate the nature, purity and crystalline/amorphous phases in the lattice of sample particles. Therefore, XRD was used to analyze the purity and crystalline nature of curcumin and nano-curcumin (Fig. 3). Very sharp intense and characteristic peaks of Cur-SM were observed at 2θ diffraction angle; 14.20°, 17.60°, 18.55°, 22.65°, 24.50°, 26.0°, and 27.55°, 35.8°. This indicated the crystalline nature of the as prepared nanoparticles of curcumin obtained from

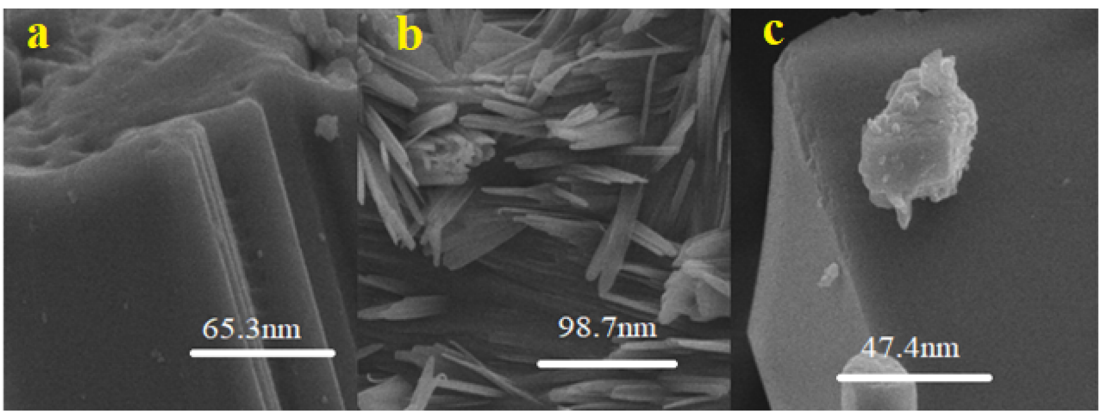

Fig. 2 Scanning electron microscopic images of nano-curcumin (a) Cur-NSM, (b) Cur-SM, and (c) Cur-ASP.

Table 1 Solubility studies of nano-curcumin

Sample	Molar absorptivity (mol^{-1} cm^{-1})	Absorbance	Concentration (mol L^{-1})	Solubility ($\mu g\ mL^{-1}$)
Cur-NSM	6.18×10^3	0.837	1.21×10^{-4}	74.0
Cur-SM	6.58×10^3	1.246	7.15×10^{-5}	46.7
Cur-ASP	6.66×10^3	1.432	2.14×10^{-4}	79.2
Curcumin	4.900×10^4	0.132	2.68×10^{-6}	0.98

sonication method whereas Cur-NSM and Cur-ASP exhibited comparatively broad characteristic peaks of curcumin on diffraction angle 2θ at 25.8°, 22.65°, 35.7°, 39.1° and 41.0°. According to the diffraction analysis, the synthesized Cur-SM is more crystalline than Cur-NSM and Cur-ASP, which have a powdered form. Using sheerer equation from the XRD spectrographs (Fig. 3), the particle size of nano-curcumin was calculated. The particles size calculated for Cur-NSM, Cur-SM and Cur-ASP was 65.3 nm, 98.7 nm, and 47.4 nm respectively. These results show a pretty good agreement with the results obtained by the SEM analysis and thus confirm the approximate size of the nano-curcumin particles.

3.2. Solubility studies of nano-curcumin in water

The solubility studies of nano-curcumin were compared with pure curcumin, molar absorptivity was used to determine the solubility of nano-curcumin in water by using Lambert–Beer law ($A = \varepsilon cl$). The results revealed that the Cur-ASP has maximum molar absorptivity which indicated its higher solubility than the Cur-NS and Cur-SM (Table 1). The reduction in particle size of curcumin increases its solubility drastically and the results of our study are inconsistent with the reported ones.[41,42]

The nano-sized curcumin particles promote dissolution due to their larger surface area and hence to increase their aqueous solubility. Some previously reported studies show similar trends too where the efficacy and solubility of nanoparticles was enhanced by reducing the particle size of the active ingredients to nanoparticles size. The reduced particles size gives rise to a better wettability because of an increased specific area and thus solubility and dissolution rate of curcumin nanoparticles increases dramatically.[10,28]

3.3. 1,1-Diphenyl-2-picrylhydrazyl (DPPH)-2,2-diphenyl-1-picrylhydrazyl free radical scavenging assay

DPPH free radical scavenging assay was employed to determine the antioxidant potential of nano-curcumin, curcumin, and standard (butylated hydroxytoluene, BHT). Free radical scavenging efficacies (Fig. 4a) of all the nano-curcumin showed a dose-dependent gradual increase at 15.0–75.0 $\mu g\ mL^{-1}$. The IC_{50} of each of nano-curcumin, curcumin, and standard were also determined (Fig. 4b). The results revealed that all the nano-curcumin and curcumin tested had a highest DPPH free radical scavenging activity at the maximum concentration (75.0 $\mu g\ mL^{-1}$). Cur-ASP showed the highest free radical scavenging potential (48.84 ± 0.98%) as compared to Cur-NSM (48.28 ± 1.45%), Cur-SM (47.33 ± 1.38%), and curcumin (45.63 ± 0.78%) at the concentration of 75 $\mu g\ mL^{-1}$ whereas BHT showed the DPPH free radical scavenging activity of 50.48 ± 1.11%.

Moreover, Cur-ASP was found to be most active nano-curcumin with an IC_{50} of 37.05 $\mu g\ mL^{-1}$ followed by Cur-SM (IC_{50} = 39.57 $\mu g\ mL^{-1}$) and Cur-NSM gave the lowest anti-free radical activity with an IC_{50} of 40.59 $\mu g\ mL^{-1}$ (Fig. 4b). For comparative purposes, BHT was used as antioxidant standards and showed an interesting anti-free radical activity with an IC_{50}

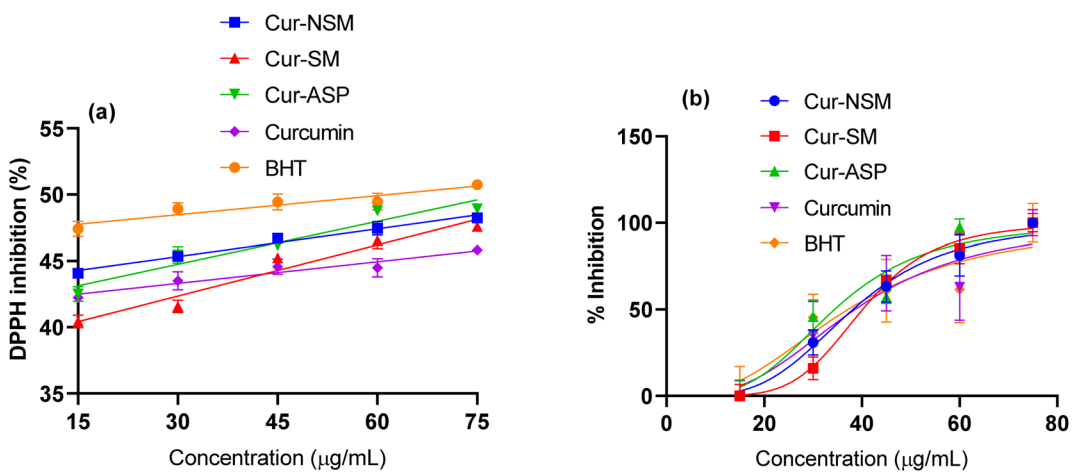

Fig. 4 1,1-Diphenyl-2-picrylhydrazyl (DPPH)-2,2-diphenyl-1-picrylhydrazyl radical scavenging activities of (a) Cur-NSM, Cur-SM, Cur-ASP, curcumin, BHT and (b) IC_{50}.

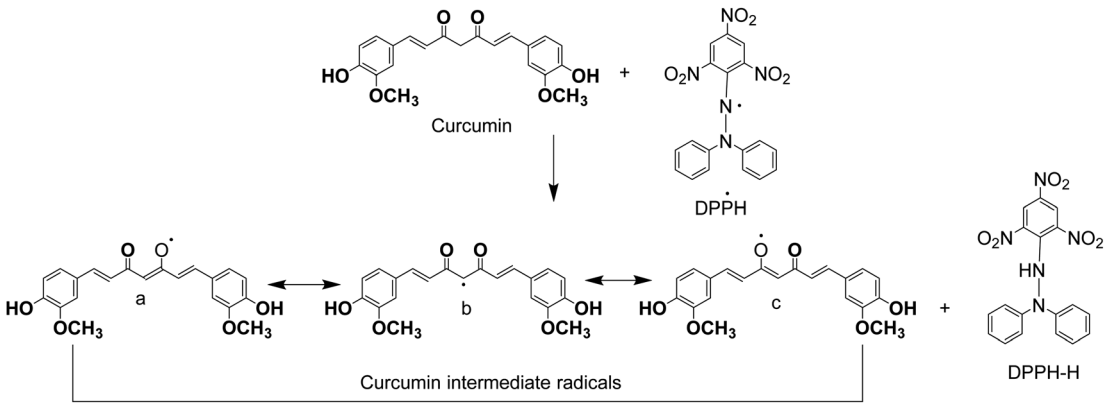

Fig. 5 Proposed reaction of curcumin with 1-diphenyl-2-picrylhydrazyl (DPPH)-2,2-diphenyl-1-picrylhydrazyl.

of 36.15 μg mL^{-1}. In our study, curcumin nanoparticles of different sizes provide increased surface area to expose the functional phenolic groups more effectively, which makes them able to effectively display their free radical scavenging ability.

Curcumin exhibits potential biological activities to fight against chronic diseases and can act on several molecular pathways. However, the antioxidant feature of curcumin is considered as the most important one. Oxidative stress is a result of an imbalance between the elimination and production of ROS and can be related to many chronic diseases and aging process.[43] The properties of curcumin responsible for the removal of reactive nitrogen and oxygen, regulation of different enzymes and metal chelation are because of the action of curcumin on markers of oxidative stress. This proves that curcumin acts as a potential antioxidant.[44] Various functional groups are present in curcumin. The phenolic functional groups trap electron to deter the production of H_2O_2 and scavenge the superoxide radicals, the β-diketo group that produces metal–ligand complexation, and carbon to carbon double bonds. Thus, the molecule shows some unique antioxidant characteristics.[45] Some researchers reported antioxidant activities of curcumin *versus* oxidative stress caused by diabetes mellitus. The study was performed on cochlear fibroblasts in rat models of diabetes mellitus and the authors concluded that an increased expression of superoxide dismutase causes curcumin to confer antioxidant protection.[46] The antiradical power of an antioxidant can be determined with the DPPH$^{\bullet}$ method by measuring a decrease in absorbance of DPPH$^{\bullet}$ at 515 nm. An antioxidant scavenges the DPPH$^{\bullet}$ by donating a hydrogen to form a stable DPPH$^{\bullet}$ molecule and the absorbance decreases as a result. The molecules, in the radical form, give an absorbance at 515 nm which disappears after acceptance of hydrogen or an electron from an antioxidant compound to become a diamagnetic stable molecule.[47]

As Fig. 5 shows, the heptadienone links between the two methoxyphenol rings contain a highly activated C-atom in the keto form of curcumin. An H-atom can easily be abstracted by curcumin from this C-atom. However, the abstraction of H-atom from the phenolic ring is much difficult because of an intramolecular H-bonding of phenolic hydrogen atoms to the adjacent methoxy groups. Theoretical calculations show that **b** is the most stable one among the intermediates (**a–c**) (Fig. 5). While the value of calculated formation energy (ΔH) for **b** is −42.05 kcal mol^{-1}, this value was found as 39.45 kcal mol^{-1} for "**a**" and 54.70 kcal mol^{-1} for "**c**". An H-atom is easily abstracted by DPPH radicals from the free hydroxyl group that is responsible for the exceptional antioxidant properties of curcumin. As a result, the reaction of DPPH radicals in alcoholic medium disappears by curcumin, while the phenolic portion of curcumin appears as an electron donor reaction site. The ability of curcumin to donate an electron is analyzed from the measurement of one-electron-transfer to DPPH radicals. The *tert*-butoxyl [$(CH_3)_3CO^{\bullet}$] radicals were also used to investigate the H-atom transfer reactions of curcumin and same results were obtained with the same mechanism observation of these radicals scavenging. In addition, the donation of hydrogen atom from β-diketone moiety to a lipid peroxyl radical or a lipid alkyl was marked as a potential antioxidant action of curcumin.[47,48]

3.4. α-Amylase inhibitory assay

Nano-curcumin, curcumin, and standard (acarbose) were subjected to α-amylase inhibitory assay. The α-amylase inhibitory values (Fig. 6a) of all the nano-curcumin showed a dose-dependent gradual increase in the concentration range of 20.0–100.0 μg mL^{-1}. The IC_{50} of each of nano-curcumin, curcumin, and standard were also determined (Table 2). The results revealed that all the nano-curcumin and curcumin tested had a highest α-amylase inhibition activity at the maximum concentration (100.0 μg mL^{-1}). Cur-ASP showed the highest α-amylase inhibition potential (68.67 ± 1.02%) as compared to Cur-NS (67.85 ± 0.45%) and Cur-SM (55.67 ± 1.11%) at the concentration of 100 μg mL^{-1}. Curcumin and acarbose showed the α-amylase inhibition of 52.84 ± 0.41% and 68.74 ± 0.28% respectively.

Cur-ASP was found to be most active nano-curcumin with an IC_{50} of 49.61 ± 0.61 μg mL^{-1} followed by Cur-SM (IC_{50} = 50.29 ± 0.78 μg mL^{-1}) and Cur-NSM gave the inhibitory activity with an IC_{50} of 51.54 ± 0.54 μg mL^{-1} (Table 2). For comparative purposes, acarbose was used as reference standards, which showed α-amylase inhibition activity with an IC_{50} of 48.57 ± 0.23 μg mL^{-1}.

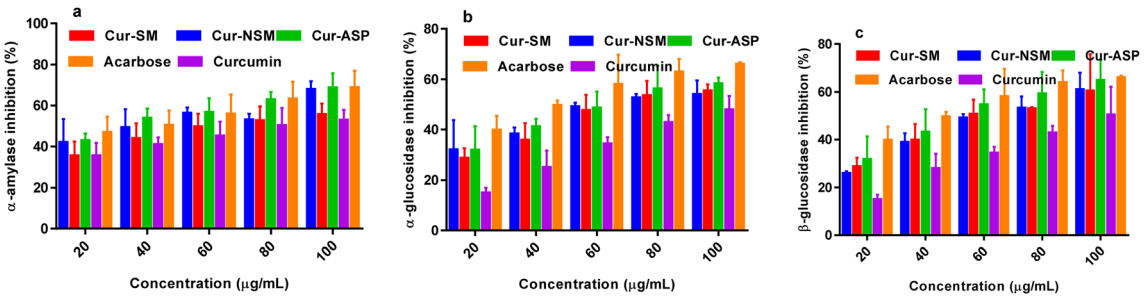

Fig. 6 α-Amylase inhibition (a) α-glucosidase inhibition (b) β-glucosidase inhibition (c) of Cur-NSM, Cur-SM, Cur-ASP, curcumin, and acarbose.

The main cause of most of the DM complications in patients is hyperglycemia. Inhibition of complex polysaccharides hydrolysis by pancreatic α-amylase is one of the most effective strategies to manage DM. Nano-curcumin is a potential agent to manage the DM because it shows excellent inhibition effect against α-amylase.[49]

3.5. α-Glucosidase inhibition assay

Nano-curcumin, curcumin, and standard (acarbose) were subjected to α-glucosidase inhibitory assay. The α-glucosidase inhibitory values (Fig. 6b) of all the nano-curcumin showed a dose-dependent gradual increase at 20.0–100.0 μg mL^{-1}. The results revealed that all the nano-curcumin and curcumin tested had a highest α-glucosidase inhibition activity at the maximum concentration (100.0 μg mL^{-1}). Cur-ASP showed the highest α-glucosidase inhibition potential (58.30 ± 0.52%) as compared to Cur-NSM (53.98 ± 1.12%) and Cur-SM (55.44 ± 1.11%) at the concentration of 100 μg mL^{-1}. Curcumin and acarbose showed α-glucosidase inhibition of 47.87 ± 0.31% and 66.04 ± 0.18% respectively. The IC_{50} of each of nano-curcumin, curcumin, and standard were also determined (Table 2). Cur-ASP was found to be most active nano-curcumin with an IC_{50} of 47.62 ± 0.48 μg mL^{-1} followed by Cur-SM (IC_{50} = 48.51 ± 0.29 μg mL^{-1}) and Cur-NSM gave the inhibitory activity with an IC_{50} of 49.10 ± 0.22 μg mL^{-1} (Table 2). For comparative purposes, acarbose was used as reference standards and showed α-glucosidase inhibition activity with an IC_{50} of 45.76 ± 0.13 μg mL^{-1}.

In glucose metabolism, α-glucosidase is highly important as it breaks α-glucopyranoside bond as well as breaks oligosaccharides and disaccharides into absorbable monosaccharide units that ultimately maintain the after meal availability of glucose and degree of postprandial hyperglycemia. Due to their site (intestine) directed action, α-glucosidase inhibitors are charming targets to develop nontoxic, safer, and potent antidiabetic agents.[50] The nano-curcumin demonstrated promising inhibition results *versus* α-glucosidase which indicates that curcumin is a potential candidate for the treatment of DM.

3.6. β-Glucosidase inhibition assay

β-Glucosidase inhibition assay was also performed for all the nano-curcumin, curcumin, and standard (acarbose). The β-glucosidase inhibitory values (Fig. 6c) of all the nano-curcumin also showed a dose-dependent gradual increase at 20.0–100.0 μg mL^{-1}. The results showed that all the nano-curcumin and curcumin tested had a highest β-glucosidase inhibition activity at the maximum concentration (100.0 μg mL^{-1}). Cur-ASP showed the highest β-glucosidase inhibition potential (64.80 ± 0.43%) as compared to Cur-NSM (60.98 ± 0.92%) and Cur-SM (60.44 ± 0.81%) at the concentration of 100 μg mL^{-1}. Curcumin and acarbose showed β-glucosidase inhibition of 50.38 ± 0.11% and 66.05 ± 0.47% respectively. The IC_{50} of each of nano-curcumin, curcumin, and standard were also determined (Table 2). Cur-ASP was found to be most active nano-curcumin with an IC_{50} of 47.13 ± 0.21 μg mL^{-1} followed by Cur-SM (IC_{50} = 49.05 ± 0.19 μg mL^{-1}) and Cur-NSM gave the inhibitory activity with an IC_{50} of 47.69 ± 0.34 μg mL^{-1} (Table 2). For comparative purposes, acarbose was used as reference standards and showed α-glucosidase inhibition activity with an IC_{50} of 45.55 ± 0.21 μg mL^{-1}.

In the human body, acidic β-glucosidase can act as a catalyst in the hydrolysis of glucosylceramide as a lysosomal enzyme. Lysosomal storage disorders can occur due to accumulation of glucosylceramide as a result of dysfunction and misfolding of the acidic β-glucosidase activity. In various cancers such as hepatocellular and breast cancers, some enhanced levels of enzyme were observed especially during advanced stages of above diseases and thus resistance of tumors increases against chemotherapy or drugs. Curcumin is a famous and powerful anticancer agent and nano-curcumin showed exceptional results to inhibit β-glucosidase. Nano-curcumin could give anticancer effects *via* targeting the β-glucosidase in the treatment of cancer.[51]

The inhibition activity is closely related to the particle size. Greater the particle size, lower will be the activity. If the particle

Table 2 IC_{50} for enzyme inhibition

	IC_{50} (μg mL^{-1}), mean ± SD		
Sample	α-Amylase	α-Glucosidase	β-Glucosidase
Cur-NSM	51.54 ± 0.54	49.10 ± 0.22	47.69 ± 0.34
Cur-SM	50.29 ± 0.78	48.51 ± 0.29	49.05 ± 0.19
Cur-ASP	49.61 ± 0.61	47.62 ± 0.48	47.13 ± 0.21
Curcumin	52.79 ± 1.02	52.61 ± 0.92	51.92 ± 0.14
Acarbose	48.57 ± 0.23	45.76 ± 0.13	45.55 ± 0.21

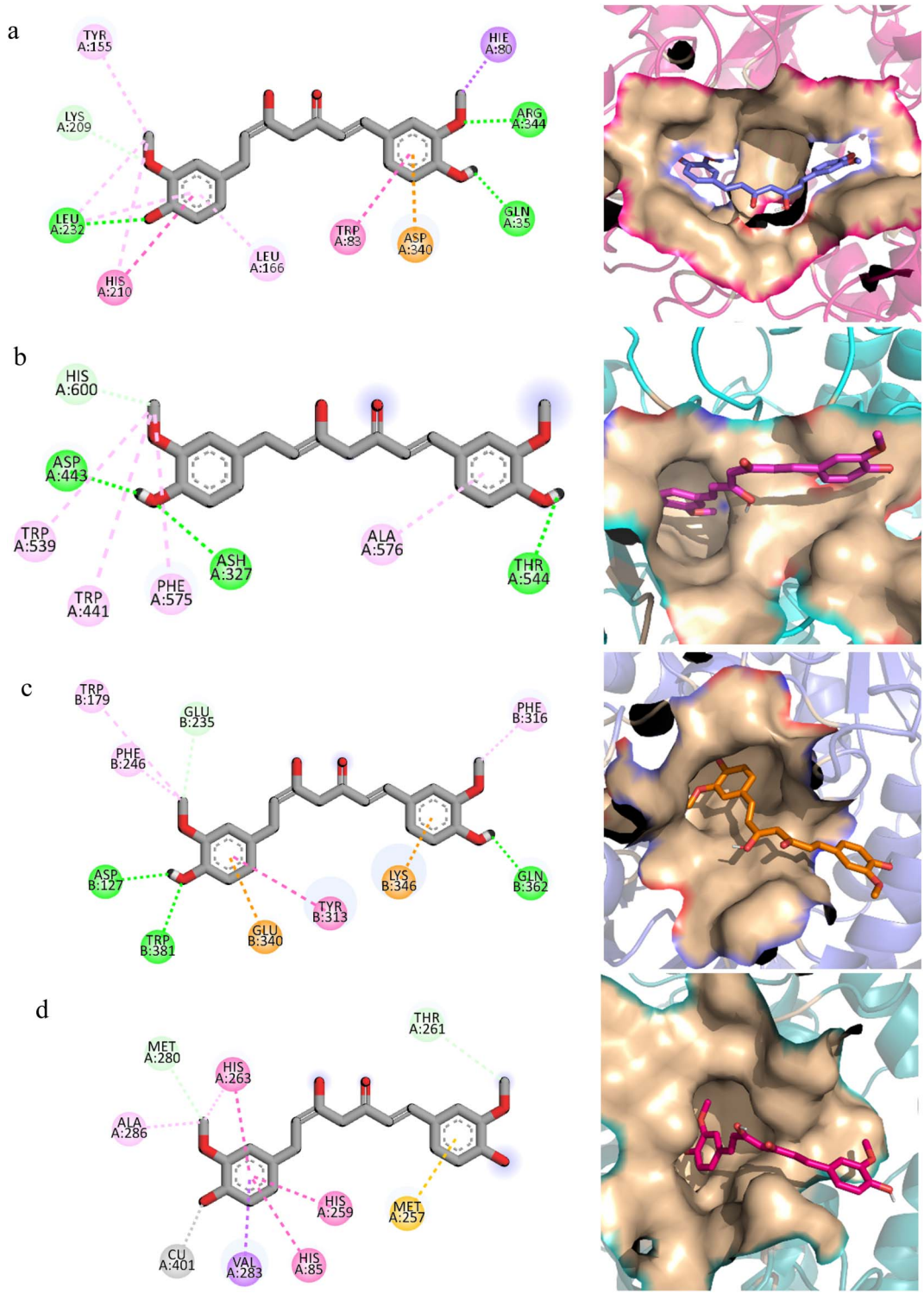

Fig. 7 The molecular interactions of curcumin with (a) α-amylase (b) α-glucosidase (c) β-glucosidase (d) polyphenol oxidase. The hydrogen bonds are shown with green color, Pi–sigma with purple, Pi–Pi stacking with pink and hydrophobic interactions with magenta color. The binding modes are shown in surface representations.

size is smaller, the surface area increases which makes the functional groups available for H-bonding become more significant while bulging on the surface and there is more opportunity for the C=O, OCH_3, OH groups present in the structure of curcumin to create more H-bonding and some other groups having hydrophobic linkage may become important to generate overall bonding in such a way it may change the symmetry of enzyme thus making it unavailable for it substrate

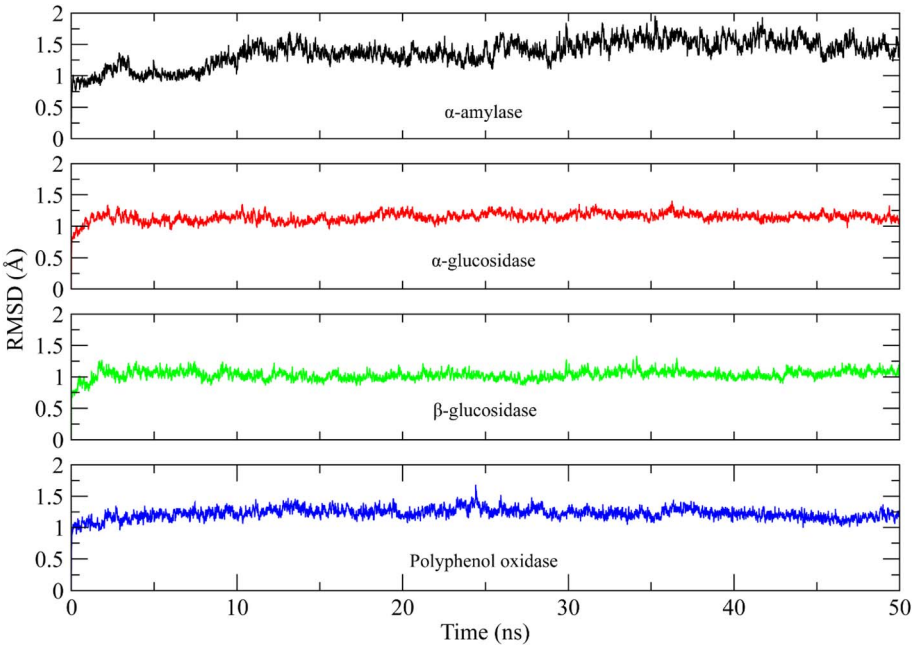

Fig. 8 The root mean square deviation plots of backbone atoms of targeted protein indicating the stable protein–ligand complex. α-Amylase (black) α-glucosidase (red) β-glucosidase (green) polyphenol oxidase (blue).

to bind and hydrolyze to release glucose to blood. In this way it is an indirect strategy to control glucose level in blood by controlling α-amylase and α-glucosidase enzyme. As well to use it as anticancer agent to control the β-glucosidase.

3.7. Molecular docking and simulation studies

The molecular interactions of curcumin with the target proteins were analyzed by docking studies. Several docked poses of curcumin were generated into the binding sites and among them, one pose was selected based on the interactions and plausible binding mode. Curcumin made 3 hydrogen bonds with Gln35, Leu232, Arg344, one Pi–sigma bond with His80, one Pi–anion bond with Asp340, and was involved in hydrophobic interactions with Trp83, Tyr155, Leu166, and His210 residues of α-amylase Fig. 7a. Similarly, curcumin made three hydrogen bonds with Ash327, Asp443, and Thr544 of α-glucosidase while

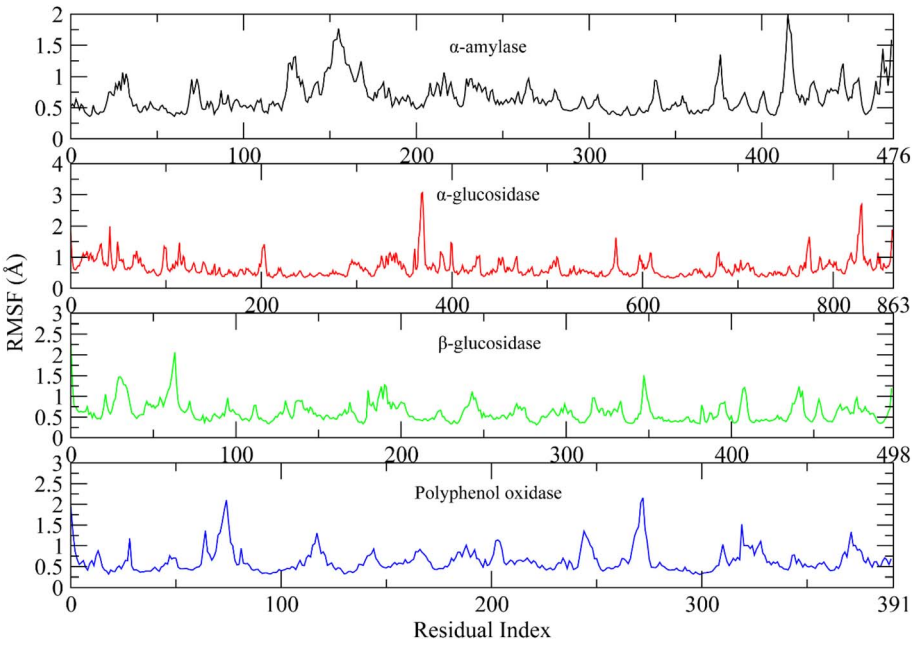

Fig. 9 The root mean square fluctuation plots of targeted proteins residues indicating the stable rigid structure of protein during simulation. α-Amylase (black) α-glucosidase (red) β-glucosidase (green) polyphenol oxidase (blue).

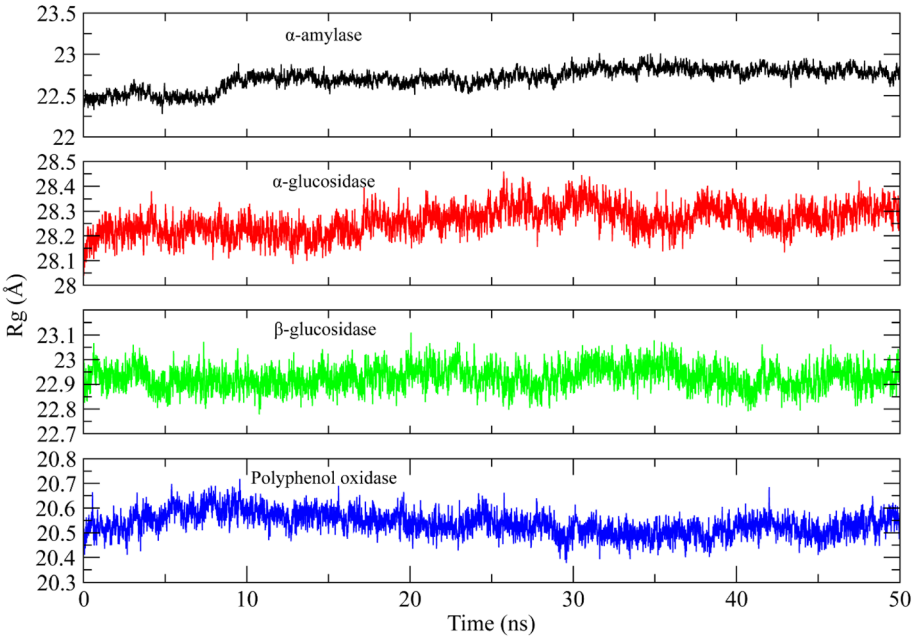

Fig. 10 The radius of gyration analysis plots of targeted protein complexes indicating the compactness of systems during simulation. α-Amylase (black) α-glucosidase (red) β-glucosidase (green) polyphenol oxidase (blue).

made four hydrophobic interactions with Trp441, Trp539, Phe575, and Ala576 Fig. 7b. In case of β-glucosidase, curcumin made 3 hydrogen bonds with Asp127, Gln362, Trp381, one Pi–Pi stacking with Tyr313, two Pi-cation and anion bonds with Glu340 and Lys346, and three hydrophobic interactions with Trp179, Phe246, and Phe310 Fig. 7c. Lastly, it one Pi–sigma bond with Val283, one Pi–sulfur bond with Met257, one hydrophobic interaction with Ala286, and three Pi–Pi stackings with His85, His259, and His 263 of polyphenol oxidase Fig. 7d.

In order to find the stability of protein–ligand complex, the RMSD of protein backbone atoms complexed with curcumin was calculated over the simulation time (Fig. 8).[52] It can be observed that three complexes (of α-glucosidase, β-glucosidase, polyphenol oxidase) equilibrated at 2 ns and then attained stability in RMSD values in the range of 1–1.25 Å throughout the simulation with minor deviations in polyphenol oxidase (green) during 20 to 25 ns where it increased to ∼1.5 Å but attained previous confirmation at 30 ns. The α-amylase complex (black) equilibrated at 5 ns and attained a value of 1 Å till ∼8 ns. The RMSD value then gradually increased to ∼1.5 Å at 10 ns and remained in the range of 1.25–1.5 Å till 30 ns. The RMSD increased to ∼2 Å after 30 ns and remained in this range till 40 ns and then attained the previous value of ∼1.25 Å during 40 to 50 ns period. The small deviations in RMSD values indicated that the complexes were stable during simulation.

The root mean square fluctuations describe the flexible residues of the protein.[53] The higher RMSF value shows the flexible regions such as loops while lower value indicates the rigid residues such as helices and sheets. The RMSF plots of studied systems are shown in Fig. 9. The RMSF plots of all complexes showed that the protein residues did not show major fluctuations. Only loop regions showed minor fluctuations. The residues from 120 to 160 and 410 to 420 showed minor fluctuations in α-amylase complex. The residues from 370 to 380 and 820 to 830 in α-glucosidase, 60 to 70 in β-glucosidase, and 70 to 80, 260 to 280 in polyphenol oxidase showed minor variations. The other residues did not show such fluctuations indicating the rigid portion of the proteins.

Similarly, the radius of gyration (R_g) was calculated to check the compactness of the protein when the ligands were bound to it.[54] The higher R_g values indicate the unfolding events in protein structure during simulation. The R_g plots of the systems are shown in Fig. 10. It can be observed that the R_g value of α-amylase complex was in range of 22.5 Å till 8 ns and then gradually increased to ∼22.75 Å at 10 ns and then remained in the same range till the end of simulation. The R_g value of α-glucosidase complex was in the range of 28.2 to 28.3 Å till 20 ns and then slightly increased to 28.4 Å during 20 to 30 ns interval and then attained the previous values during 35 to 50 ns. The R_g value of β-glucosidase was remained in the range of 22.9 to 23 Å throughout the simulation time. Lastly, the R_g value of polyphenol oxidase complex was high in first 20 ns as compared to last 30 ns and attained a value in range of 20.5 Å towards the end of simulation. The stable R_g values showed that the proteins did not undergo any unfolding event during simulation when bound to the curcumin.

4. Conclusion

Curcumin is nontoxic and very cost-effective polyphenol with wide range of medicinal properties. It is extracted from curcuma longa. Several *in vitro*, *in vivo*, and clinical trial investigations reported in literature have provided evidence for the bioactive role of curcumin in the prevention and treatment of

various human diseases. Curcumin nano-formulations have markedly exhibited their potential in inhibition of the enzymes responsible for diabetic mellitus. A structure activity relationship has been established using molecular docking studies for the relation of alpha amylase and alpha glucosidase enzymes inhibition with that of curcumin. Cur-ASP has smaller size (47.4 nm) than that of Cur-MS (98.7 nm) and Cur-NSM (65 nm). It has inhibited the DPPH free radical, and all three enzymes responsible for diabetes. It means that smaller the size, more surface is exposed with functional groups would be provided which has more opportunity to bind and inhibit the binding sites of enzymes more easily as compared to the native curcumin. It has been confirmed that curcumin nano-formulations improve curcumin bioavailability by enhancing its water solubility and are systemically safe. It would be more available to biological system when more soluble in water. However, testing of these formulations as therapeutic modalities is highly desirable and is crucial for future clinical trials and for human use. In addition, implementation of curcumin nano-formulations as enzyme inhibitors exhibited even more than parallel inhibition results to that of the standard drug used. In present study, we have shown the alpha-amylase inhibition (AAI) as well as α glucosidase inhibition and antioxidant activity of pure and modified curcumin for the treatment of DM. Curcumin being a magical molecule exhibited a promising antioxidant as well as antidiabetic potential that can be explored in the development of novel drugs for oxidative stress-related diabetes management. A weak AAI suggests other possible therapeutic targets in the management of DM. Our studies partially confirmed the traditional use of curcumin modified to different nano-sizes using different fabrication techniques to enhance its water solubility and thus bioavailability for diabetes management in the region. Since the oxidative stress has a key role in the development of DM. Increased oxidative species production and reduced antioxidant capacity have been repeatedly shown in subjects with DM. Owing to detrimental effects of oxidative stress on the development of DM and the progression of its vascular complications, antioxidant therapy has been considered a potentially effective approach to treat the DM. Further, the molecular docking studies revealed that the plausible binding modes of curcumin with α-amylase, α-glucosidase, β-glucosidase, and polyphenol oxidase showed better molecular interactions and make stable complexes with the studied enzymes when explored by 50 ns long MD simulation.

Data availability

All data generated or analysed during this study are included in this published article.

Conflicts of interest

The authors declare no conflict of interest.

Acknowledgements

The authors received no specific funding for this work.

References

1 M. Ahmed, A. Khaleeq, R. Huma and S. Munir, *Spectrosc. Lett.*, 2017, **50**, 432–439.
2 M. Ahmed, M. A. Qadir, M. I. Shafiq, M. Muddassar, Z. Q. Samra and A. Hameed, *Arabian J. Chem.*, 2019, **12**, 41–53.
3 M. Ahmed, M. A. Qadir, M. I. Shafiq, M. Muddassar, A. Hameed, M. N. Arshad and A. M. Asiri, *Acta Pharm.*, 2017, **67**, 385–395.
4 M. Ahmed, M. A. Qadir, A. Hameed, M. Imran and M. Muddassar, *Chem. Biol. Drug Des.*, 2018, **91**, 338–343.
5 M. Ahmed, M. A. Qadir, A. Hameed, M. N. Arshad, A. M. Asiri and M. Muddassar, *Bioorg. Chem.*, 2018, **76**, 218–227.
6 G. H. Shin, J. Li, J. H. Cho, J. T. Kim and H. J. Park, *J. Food Sci.*, 2016, **81**, N494–N501.
7 M. Ahmed, M. A. Qadir, A. Hameed, M. N. Arshad, A. M. Asiri and M. Muddassar, *Biochem. Biophys. Res. Commun.*, 2017, **490**, 434–440.
8 M. Ahmed, M. A. Qadir and M. I. Shafiq, *Lat. Am. J. Pharm.*, 2017, **36**, 1789–1795.
9 M. Ahmed, S. Ahmad and M. Irfan, *Sep. Sci. Plus*, 2021, **4**, 118–127.
10 R. K. Basniwal, H. S. Buttar, V. Jain and N. Jain, *J. Agric. Food Chem.*, 2011, **59**, 2056–2061.
11 T. Gupta, J. Singh, S. Kaur, S. Sandhu, G. Singh and I. P. Kaur, *Front. bioeng. biotechnol.*, 2020, **8**, 879.
12 H. Yavarpour-Bali, M. Ghasemi-Kasman and M. Pirzadeh, *Int. J. Nanomed.*, 2019, **14**, 4449.
13 A. Ubeyitogullari and O. N. Ciftci, *Sci. Rep.*, 2019, **9**, 1–11.
14 G. M. Abu-Taweel, M. F. Attia, J. Hussein, E. M. Mekawi, H. M. Galal, E. I. Ahmed, A. A. Allam and M. E. El-Naggar, *Biomed. Pharmacother.*, 2020, **131**, 110688.
15 L.-J. Yan, *J. Diabetes Res.*, 2014, **2014**, 137919.
16 F. Zaccardi, D. R. Webb, T. Yates and M. J. Davies, *Postgrad. Med. J.*, 2016, **92**, 63–69.
17 D. E. Ejike, M. A. Adam, O. S. Sheu, P. Nganda, E. Iliya, D. A. Moses and O. O. Alfred, *J. Diabetes Endocrinol.*, 2018, **9**, 11–19.
18 A. A. Oroojan, N. Chenani and M. An'aam, *Int. J. Hepatol.*, 2020, **2020**, 5890378.
19 V. Solmaz, H. Köse Özlece, H. A. Eroglu, H. Aktuğ, O. Erbaş and D. Taşkıran, *Neurol. Res. Int.*, 2017, **2017**, 5952149.
20 R. P. Robertson and J. S. Harmon, *FEBS Lett.*, 2007, **581**, 3743–3748.
21 P. Dandekar, S. Ramkumar and A. RaviKumar, *Stud. Nat. Prod. Chem.*, 2021, **70**, 381–410.
22 L. Sim, K. Jayakanthan, S. Mohan, R. Nasi, B. D. Johnston, B. M. Pinto and D. R. Rose, *Biochemistry*, 2010, **49**, 443–451.
23 J. Wu, B. Hu, S. Lu, R. Duan, H. Deng, L. Li, L. He, Y. Zhao, J. Wang and Z. Yu, *Carbohydr. Res.*, 2022, **511**, 108478.
24 B. Salehi, A. Ata, N. V. Anil Kumar, F. Sharopov, K. Ramirez-Alarcon, A. Ruiz-Ortega, S. Abdulmajid Ayatollahi, P. Valere Tsouh Fokou, F. Kobarfard and Z. Amiruddin Zakaria, *Biomolecules*, 2019, **9**, 551.

25 Y. Naveen, A. Urooj and K. Byrappa, *J. Herb. Med.*, 2021, **28**, 100436.
26 M. M. Yallapu, P. K. B. Nagesh, M. Jaggi and S. C. Chauhan, *AAPS J.*, 2015, **17**, 1341–1356.
27 M. Kakran, N. G. Sahoo, I.-L. Tan and L. Li, *J. Nanopart. Res.*, 2012, **14**, 1–11.
28 S. S. Hettiarachchi, S. P. Dunuweera, A. N. Dunuweera and R. G. Rajapakse, *ACS Omega*, 2021, **6**, 8246–8252.
29 M. Ahmed, M. Imtiaz Shafiq, A. Khaleeq, R. Huma, M. Abdul Qadir, A. Khalid, A. Ali and A. Samad, *J. Chem.*, 2016, **2016**, 8072305–8072310.
30 M. Ahmed, A. Khaleeq and S. Ahmad, *World Appl. Sci. J.*, 2014, **30**, 1664–1667.
31 M. Ahmed, S. K. Shahzadi, M. A. Qadir, A. I. Durrani, S. Ahmad, I. KHAN, A. Munir and A. Khaleeq, *Lat. Am. J. Pharm.*, 2020, **39**, 372–375.
32 M. Ezati, F. Ghavamipour, H. Adibi, K. Pouraghajan, S. S. Arab, R. H. Sajedi and R. Khodarahmi, *Spectrochim. Acta, Part A*, 2022, 121806.
33 L. J. S. S. Schrödinger, *Schrödinger*, LLC, New York, NY, 2017, 2017(2), pp. 2017–2011.
34 M. O. Kim, S. E. Nichols, Y. Wang and J. A. J. McCammon, *J. Comput. Aided Mol. Des.*, 2013, **27**, 235–246.
35 W. Humphrey, A. Dalke and K. J. J. Schulten, *J. Mol. Graph.*, 1996, **14**, 33–38.
36 J. C. Phillips, D. J. Hardy, J. D. Maia, J. E. Stone, J. V. Ribeiro, R. C. Bernardi, R. Buch, G. Fiorin, J. Hénin and W. J. T. Jiang, *J. Chem. Phys.*, 2020, **153**, 044130.
37 D. A. Case, H. M. Aktulga, K. Belfon, I. Ben-Shalom, S. R. Brozell, D. Cerutti, T. Cheatham, V. W. D. Cruzeiro, T. Darden and R. E. Duke, *Amber 2021: Reference Manual*, 2021.
38 W. Jorgensen and J. J. J. C. P. Chandrasekhar, *J. Chem. Phys.*, 1983, **79**, 926.
39 Y. Duan, C. Wu, S. Chowdhury, M. C. Lee, G. Xiong, W. Zhang, R. Yang, P. Cieplak, R. Luo and T. J. Lee, *J. Comput. Chem.*, 2003, **24**, 1999–2012.
40 B. J. Grant, L. Skjærven and X. Q. J. P. S. Yao, *Protein Sci.*, 2021, **30**, 20–30.
41 S. Alam, J. J. Panda and V. S. Chauhan, *Int. J. Nanomedicine*, 2012, **7**, 4207.
42 M. Ghosh, A. T. Singh, W. Xu, T. Sulchek, L. I. Gordon and R. O. Ryan, *Nanomedicine*, 2011, **7**, 162–167.
43 M. Pulido-Moran, J. Moreno-Fernandez, C. Ramirez-Tortosa and M. Ramirez-Tortosa, *Molecules*, 2016, **21**, 264.
44 K. Jakubczyk, A. Drużga, J. Katarzyna and K. Skonieczna-Żydecka, *Antioxidants*, 2020, **9**, 1092.
45 G. C. Jagetia and G. K. Rajanikant, *Antioxidants*, 2015, **4**, 25–41.
46 M. L. Del Prado-Audelo, I. H. Caballero-Florán, J. A. Meza-Toledo, N. Mendoza-Muñoz, M. González-Torres, B. Florán, H. Cortés and G. Leyva-Gómez, *Biomolecules*, 2019, **9**, 56.
47 T. Ak and İ. Gülçin, *Chem.-Biol. Interact.*, 2008, **174**, 27–37.
48 S. M. Abbas, N. Ahmad, U. A. Rana, S. U.-D. Khan, S. Hussain and K.-W. Nam, *Electrochim. Acta*, 2016, **212**, 260–269.
49 D. Stojkovic, M. Smiljkovic, A. Ciric, J. Glamoclija, L. Van Griensven, I. C. Ferreira and M. Sokovic, *S. Afr. J. Bot.*, 2019, **120**, 100–103.
50 A. Mushtaq, U. Azam, S. Mehreen and M. M. Naseer, *Eur. J. Med. Chem.*, 2023, **249**, 115119.
51 X. Liu, F. Li, L. Su, M. Wang, T. Jia, X. Xu, X. Li, C. Wei, C. Luo and S. Chen, *Bioorg. Chem.*, 2022, **127**, 106016.
52 K. Sargsyan, C. Grauffel and C. Lim, *J. Chem. Theory Comput.*, 2017, **13**, 1518–1524.
53 R. Martinez, A. Blasina, J. F. Hallin, W. Hu, I. Rymer, J. Fan, R. L. Hoffman, S. Murphy, M. Marx and G. Yanochko, *PLoS One*, 2015, **10**, e0138616.
54 M. Y. Lobanov, N. Bogatyreva and O. J. M. B. Galzitskaya, *Mol. Biol.*, 2008, **42**, 623–628.